District-scale mapping of Mississippi Valley-type Pb-Zn mineralisation potential through an AHP-TOPSIS model: a case study from the southern Hamedan area (western Iran)

S. Darabi[1], H.A. Haroni[2,3] and M.A. Aliabadi[1]

[1] Earth Science department, Mahallat branch, Islamic Azad University, Mahallat, Iran
[2] Centre for Exploration Targeting, Australian Research Council Centre of Excellence for Core to Crust Fluid Systems, School of Earth and Environment, the University of Western Australia, Crawley, Australia
[3] Department of Mining Engineering, Isfahan University of Technology, Isfahan, Iran

ABSTRACT   The southern Hamedan area in western Iran is a region with high potential for Mississippi Valley type Pb-Zn mineralisation, for which a suitable prospecting map is needed to optimise future mineral exploration. Satellite imagery, geologic and geochemical data sets of the area were used to map Pb-Zn mineralisation potential using the analytical hierarchy process and the technique of order preference by similarity to the ideal solution (AHP-TOPSIS). Various criteria maps representing specific Pb-Zn criteria, such as lithological classes, structural controls, hydrothermal alteration, and geochemical anomalies in the Pb and Zn catchment basin geochemical anomalies, were integrated using the AHP-TOPSIS approach to obtain a final favourable map of Pb-Zn mineralisation in the southern Hamedan area. Fractal analysis was used to classify the final potential map into three zones: highly favourable, favourable, and slightly favourable. The four known Pb-Zn deposits are located in or adjacent to the highly favourable pixels. It is recommended that the unexplored highly favourable and favourable zones be considered for further exploration.

Key words: mineral potential mapping, Pb-Zn mineralisation, AHP-TOPSIS, western Iran.

1. Introduction

In mineral exploration, the main objective is to find new deposits in the study area. The most important steps in mineral exploration are to identify areas with high potential.

In this context, various exploration information such as satellite imagery, geological maps, geochemical anomaly maps, and geophysical signatures must be integrated to find areas of high mineralisation potential. Since the objective of mineral potential mapping (MPM) is to produce a predictive map based on several different exploration criteria, it can be considered as a multi-criteria decision-making problem (Bonham-Carter, 1994; Carranza *et al.*, 2008; Abedi *et al.*, 2012a; Ghezelbash and Maghsoudi, 2018).

In recent years, various data integration algorithms have been introduced and applied by different researchers, which can be divided into data-driven and knowledge-driven categories. In data-driven algorithms, known mineralisation indices of the study area are considered as training

data locations to investigate the relationships between mineralisation and evidential layers. Weight of Evidence (Asadi and Hale, 2001; Ford *et al.*, 2016), Support Vector Machine (Abedi *et al.*, 2012a; Geranian *et al.*, 2016), Random Forests (Carranza and Laborte, 2015a, 2015b, 2015c; McKay and Harris, 2016), logistic regression (Agterberg and Bonham-Carter, 1999; Carranza and Hale, 2001), and artificial neural networks (Porwal *et al.*, 2003b; Abedi and Nouruzi, 2012) are the best examples of data-driven algorithms.

In areas with less exploration activities, the amount of training data is not substantial and, therefore, the use of knowledge-based methods is appropriate. In such methods, exploratory evidential layers such as geological, geochemical, geophysical, and remote sensing criteria are weighted and integrated based on the opinions of geology experts (Carranza, 2011; Ghezelbash and Maghsoudi, 2018). The most common knowledge-based methods include: index overlay (Bonham-Carter *et al.*, 1990; Carranza *et al.*, 1999; Yousefi and Carranza, 2015) and fuzzy logic (An *et al.*, 1991; Porwal *et al.*, 2003a; Abedi *et al.*, 2013a, 2013b).

Since mineral potential modelling produces a favourability map based on the integration of multiple exploration data obtained from different sources of information, it can be considered as a Multi-Criteria Decision Making (MCDM) problem (Abedi *et al.*, 2012a, 2012b, 2013a, 2013b). In recent years, various MCDM algorithms have been used as knowledge-based methods, such as the analytical hierarchy process (Hosseinali and Alesheikh, 2008; Pazand *et al.*, 2011; Abedi *et al.*, 2013b), ELimination and Choice Translating REality (ELECTRE) algorithm (Abedi *et al.*, 2012a), Preference Ranking Organisation METHod for Enrichment Evaluation (PROMETHEE) algorithm (Abedi *et al.*, 2012b) and the Technique for Order of Preference by Similarity to Ideal Solution [TOPSIS (Pazand *et al.*, 2012)] as tools for mineral potential mapping.

In this paper, an integrated Analytic Hierarchy Process TOPSIS (AHP-TOPSIS) algorithm introduced by Pazand and Hezarkhani (2015) was used to map the potential of Mississippi Valley-type (MVT) Pb-Zn mineralisation in a relatively unexplored area in western Iran. The AHP-TOPSIS strategy is chosen because it has successfully been used in district-scale mineral potential mapping in recent researches (Asadi *et al.*, 2016). In addition, AHP-TOPSIS offers some compositional advantages. It is not a pure knowledge-driven or data-driven method, but a hybrid method. Similar to knowledge-driven methods, a criteria weight vector is required, but no inference system is used. Comparable to data-driven methods such as fuzzy c-means clustering, the ranking approach is based on the distance of alternatives to positive and negative ideals. The AHP-TOPSIS only needs the comparison matrix as input information to obtain the criteria weight vector, while other knowledge-based methods need more primary information.

The main parts of this study are as follows: first, the background of the data integration algorithm used, AHP-TOPSIS, is presented. Then, the prepared exploration criteria are outlined. Finally, the results of data integration modelling are presented and discussed.

2. Methodology

The AHP-TOPSIS algorithm consists of two basic steps. In the first step, the importance weight of the exploration criteria is determined from the AHP. In the next step, the TOPSIS algorithm is used to integrate the various information layers. The details of the AHP and TOPSIS algorithms are presented in the following sections.

2.1. AHP

The AHP algorithm was first introduced by Saaty (1977, 1980, 1994). It considers a decision-making problem as a hierarchical structure with elements and levels. The first level of the AHP structure is the final objective of the problem, which is an MCDM map, and the next levels are consistent with criteria and sub-criteria. To calculate the weights of the criteria, a pairwise comparison matrix should be created in which the components of each level are compared in pairs with a specific component at a higher level. To construct the comparison matrix in the AHP procedure, the pairwise comparison scale with real numbers from 1 to 9 (Table 1) was first introduced by Saaty (1997).

Table 1 - Ratio scales from 1 to 9 in the AHP procedure (from Saaty, 1977).

Number of elements	3	4	5	6	7	8	9	10	11	12	13
RI	0.52	0.89	1.11	1.25	1.35	1.4	1.45	1.49	1.51	1.54	1.56

The pairwise comparison matrix (A) for n criteria $\{c_1, c_2, c_3, ..., c_n\}$ within the second level, with regard to the ultimate goal, is prepared as:

$$A = \begin{bmatrix} a_{11} & a_{12} & ... & a_{1n} \\ a_{21} & a_{22} & ... & a_{2n} \\ ... & ... & ... & ... \\ a_{n1} & a_{n2} & ... & a_{nn} \end{bmatrix} \tag{1}$$

where a_{ij} refers to the pairwise comparison between the components i and j of a level with regard to the upper level. The elements a_{ij} are controlled by the following constrains:

$$a_{ij} > 0; \quad a_{ij} = \frac{1}{a_{ji}}; \quad a_{ii} = 1 \: \forall \: i. \tag{2}$$

Researchers have presented various approaches for determining the weights of vectors from the pairwise comparison matrix A, of which the eigenvalue approach proposed by Saaty (1977, 1980) is the most convenient. In the eigenvalue approach, the weights are determined based on the eigenvector w of the matrix A:

$$Aw = \lambda_{max}w. \tag{3}$$

In this approach, the vector for the weights of the elements is obtained by normalizing w. λ_{max} is the largest eigenvalue of the matrix A. The pairwise comparison must satisfy the transitivity expectations of pairwise comparisons. That is, it must satisfy the following relation condition:

$$a_{ij} = a_{ik} \times a_{kj}; \quad \forall \: i, j, k. \tag{4}$$

The consistency of the comparison matrix can be examined by the consistency ratio (CR),

which can be calculated by the following equation:

$$CR = \frac{CI}{RI}$$

(5)

where *RI* is known as the random index and *CI* is known as the consistency index. It is recommended that *CR* < 0.1 is allowed (Asadi *et al.*, 2016). The average *RI* values are suggested by Saaty (1980, 2001) and are shown in Table 2. The *CI* value for an *n×n* matrix is calculated by the following equation:

$$CI = \frac{\lambda_{max} - n}{n - 1}$$

(6)

Table 2 - Values of RI for different numbers of elements of the comparison matrix (Tzeng and Huang, 2011).

Number of elements	3	4	5	6	7	8	9	10	11	12	13
RI	0.52	0.89	1.11	1.25	1.35	1.4	1.45	1.49	1.51	1.54	1.56

2.2. TOPSIS

Among the proposed solution methods for MCDM problems, TOPSIS is a popular algorithm first introduced by Hwang and Yoon (1981) and, then, further developed by Lai *et al.* (1994) and Yoon and Hwang (1995). It is a straightforward algorithm that only requires weights as input from the operator (Opricovic and Tzeng, 2004; Jahanshahloo *et al.*, 2006; Tzeng and Huang, 2011), which are determined by the AHP method in this work, as explained in the previous section. The main steps of the TOPSIS algorithm are as follows (Hwang and Yoon, 1981; Jahanshahloo *et al.*, 2006; Tzeng and Huang, 2011):

1. construct a ranking decision matrix with the structure as follows:

$$A = \begin{matrix} A_1 \\ A_2 \\ . \\ . \\ A_i \\ . \\ A_m \end{matrix} \begin{bmatrix} g_{11} & g_{12} & \cdots & g_{1j} & \cdots & g_{1n} \\ g_{21} & g_{22} & \cdots & g_{2j} & \cdots & g_{2n} \\ . & . & \cdots & . & \cdots & . \\ . & . & \cdots & . & \cdots & . \\ g_{i1} & g_{i2} & \cdots & g_{ij} & \cdots & g_{in} \\ . & . & . & . & \cdots & . \\ g_{m1} & g_{m2} & \cdots & g_{mj} & \cdots & g_{mn} \end{bmatrix}$$

(7)

where A_i defines the alternatives *i, i* = 1, 2, 3, …., *m*; c_j shows *j*th criterion, *j* = 1, 2, …, *n*, belonged to *i*th alternative; and g^{ij} is a certain value denoting the efficiency rating of each alternative A_i related to each criterion c_j;

2. normalise the decision matrix. The normalised value (r_{ij}) can be calculated as follows:

$$r_{ij} = \frac{g_{ij}}{\sqrt{\sum_{i=1}^{m} g_{ij}^2}}; \quad i = 1, 2, …, m; \quad j = 1, 2, …, n;$$

(8)

3. determine the weighted normalised decision matrix with v_{ij} values as follows:

$$v_{ij} = w_{ij} r_{ij}; \quad i = 1, 2, \dots, m; \quad j = 1, 2, \dots, n; \quad \sum_{j=1}^{n} w_j = 1; \tag{9}$$

4. calculate the positive ideal and negative ideal solutions through the following equations:

$$A^* = \{v_1^*, \dots, v_n^*\} = \left\{ \left(\max_i v_{ij} | j \in J' \right), \left(\min_j v_{ij} | j \in J'' \right) \right\} \tag{10}$$

$$A^- = \{v_1^-, \dots, v_n^-\} = \left\{ \left(\min_i v_{ij} | j \in J' \right), \left(\max_j v_{ij} | j \in J'' \right) \right\} \tag{11}$$

where J' is the benefit features and J'' is the cost features;

5. calculate the individual alternatives from the ideal solution and the negative ideal solution through the Euclidean distance as follows:

$$D_i^* = \sqrt{\sum_{j=1}^{n} \left(v_{ij} - v_j^* \right)^2}; \quad i = 1, 2, \dots, m \tag{12}$$

$$D_i^- = \sqrt{\sum_{j=1}^{n} \left(v_{ij} - v_j^- \right)^2}; \quad i = 1, 2, \dots, m. \tag{13}$$

The relative similarity/closeness (RC) to the ideal solution can be determined with the following equation:

$$RC = \frac{D_i^-}{(D_i^- + D_i^+)}, \quad i = 1, 2, \dots, m. \tag{14}$$

sorting the alternatives according to their relative proximity to ideal solution. The most favourable alternative is the one that has the highest RC.

3. Study area and exploration keys

The case study with an area of about 3500 km² is located between 48°02′ and 49°12′ E longitude and 33°59′ and 34°55′ N latitude. The study area, located in the southern province of Hamedan in western Iran (Fig. 1), is a part of the Sanandaj-Sirjan tectonic belt. The Hamedan city is located in the north-eastern edge of the study area, and its aerial distance to the centre of the study area is about 40 km.

On the other hand, part of the Irankuh-Emarate Pb-Zn MVT belt presented by Karimpour and Sadeghi (2018) is located in the study area, which is an important MVT Pb-Zn mineralisation area in Iran. Based on the mineral exploration findings obtained from the detected Pb-Zn MVT indices in this belt, a set of criterion levels was selected as follows.
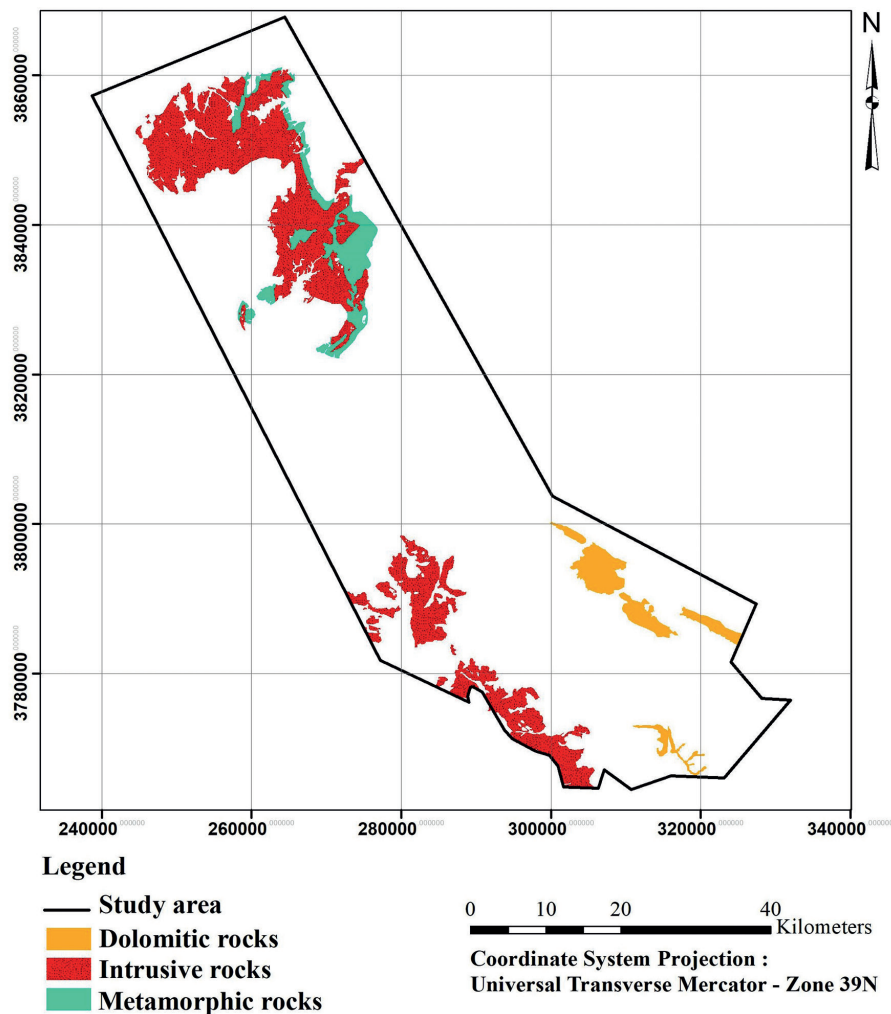
Fig. 1 - Location of the study area from satellite images.

3.1. Lithology

The known MVT deposits in the Irankuh-Emarate belt are mainly hosted on Lower Cretaceous to Cretaceous dolomitic rocks with multiple mineralisation phases (Karimpour and Sadeghi, 2018; Rajabi *et al.*, 2019). Based on the above information, the three important criteria were extracted from a geological map of the study area at a scale of 1:100,000 include dolomitic rocks, contact metamorphic rocks and intrusive igneous rocks.

3.2. Faults

The detailed studies on the structural control of the proven MVT deposits in the Emarate-Irankuh belt show that the mineralisation of these deposits is strongly influenced by normal and reverse faults (Yarmohammadi, 2015; Boveirii Konari, 2016; Mahmoodi *et al.*, 2018; Movahednia *et al.*, 2018; Peernajmodin, 2018). Based on fault lines extracted from the geological map of the study area, a raster fault density map was created and considered as a criteria map (Fig. 3).
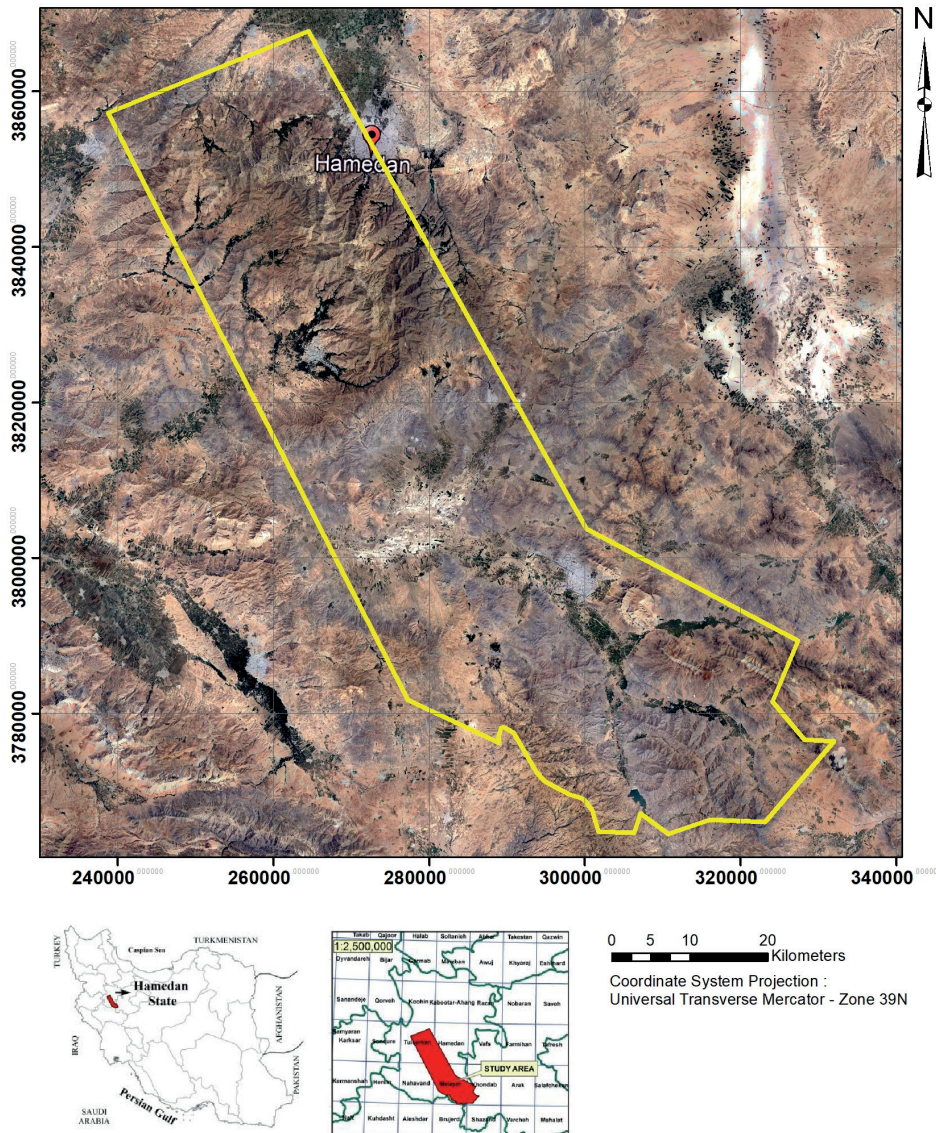
Fig. 2 - Geological map of the study area scale of 1:100,000.

3.3. Alteration

Silicified rocks, hydrothermal alteration, and Fe-rich zones are the main alterations observed in the known deposits in the Emarate-Irankuh belt (Ehya *et al.*, 2010; Mahmoodi *et al.*, 2018; Peernajmodin, 2018; Niroomand *et al.*, 2019).

Minerals associated with these alteration zones exhibit spectral absorption features in the visible near-infrared (VNIR), shortwave infrared (SWIR), and thermal infrared. The advanced space-borne thermal emission and Reflection Radiometer (ASTER) is used in this study to map alteration zones. The Aster imagery covers the VNIR (0.52-0.86 µm), SWIR (1.60-2.43 µm), and thermal infrared (TIR) (8.125-11.65 µm) spectral regions with 14 bands and high spatial (15 for VNIR, 30 for SWIR, and 90 m for TIR), spectral, and radiometric resolution (Pournamdari *et al.*,
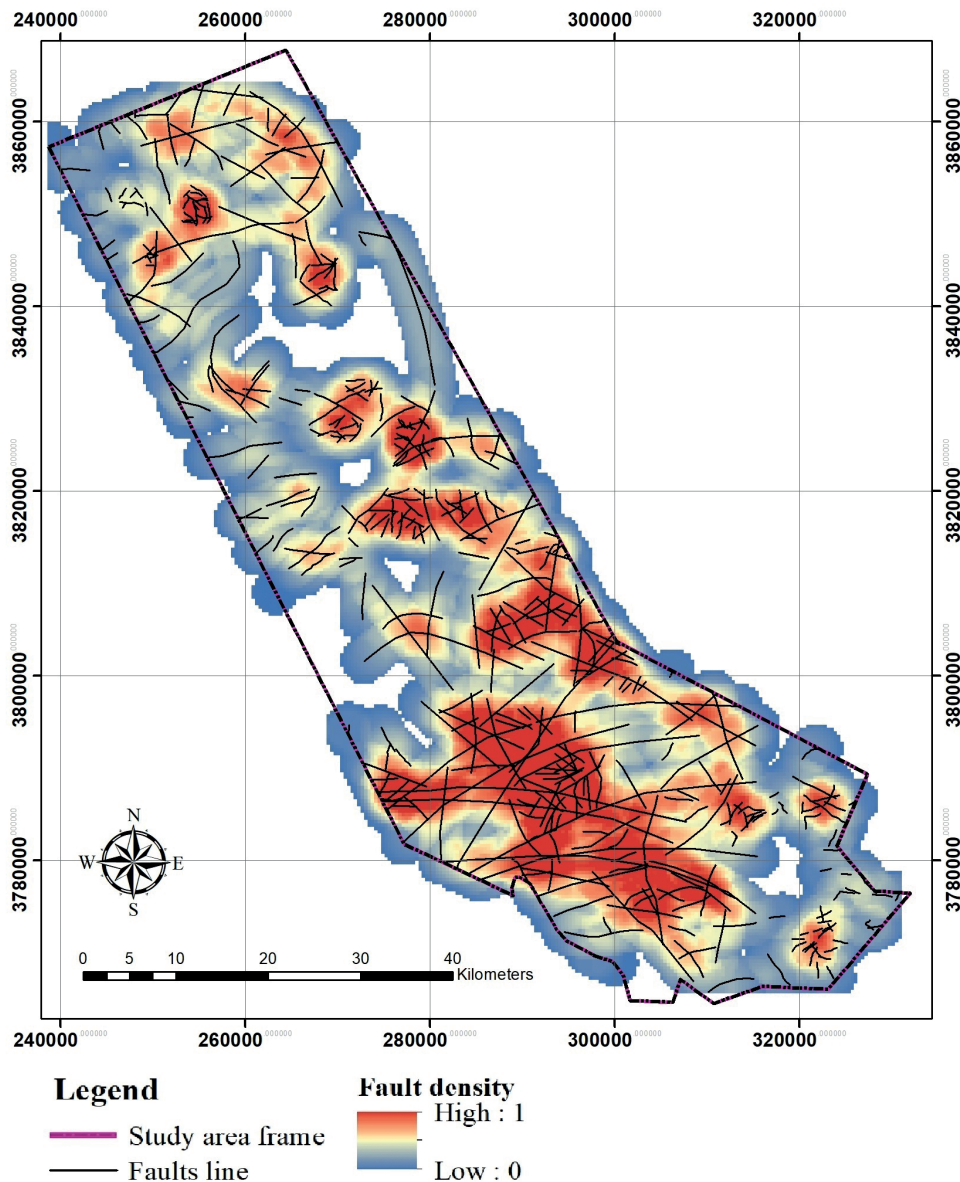
Fig. 3 - Lineament density map of the study area.

2014). The ASTER VNIR bands can be used to detect transition metals such as Fe oxide; the ASTER SWIR channels are important sources of spectral information on Al-OH, Fe-OH, Mg-OH, H-O-H and CO^3 minerals that can be used to detect argillic alteration, and the bands of ASTER TIR can be used to detect silicification zones (Amos and Greenbaum, 1989; Shahriari *et al.*, 2013). The Spectral Angle Mapper (SAM) algorithm is applied to the ASTER image to create an alteration map of the case study area. SAM is a supervised classification method that calculates the angle between the image spectra and the reference spectra (Galvão *et al.*, 2005; Gabr *et al.*, 2010; Honarmand *et al.*, 2012; Feizi and Mansuri, 2013). The United States Geological Survey (USGS) spectral library was used to select VNIR, SWIR and TIR reference spectra of iron oxide, argillic alteration, propylitic alteration, and silicified rocks (Fig. 4).
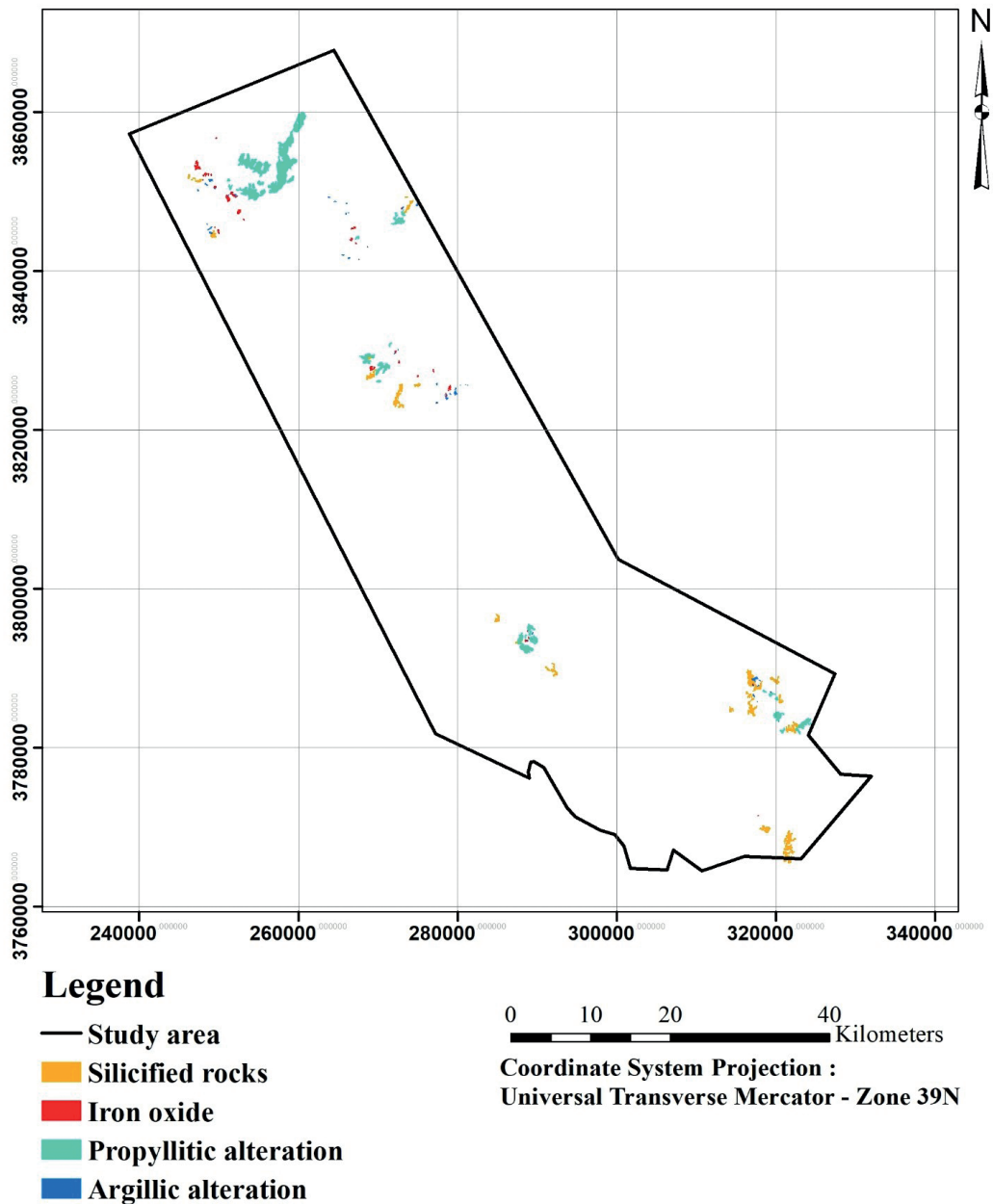
Fig. 4 - Hydrothermal alterations mapped from analysis of Landsat ETM+ and ASTER satellite data.

3.4. Geochemistry

1200 stream sediment samples were collected in the study area and analysed by the Geological Survey of Iran using the ICP method at the scale of 1:100,000. The average sampling distance is about 1.5 km. A pattern catchment analysis approach was applied to these stream sediment geochemical data to produce the raster maps of Pb and Zn geochemical anomalies. By considering the local Clark values of the Pb and Zn variables equal to 220 and 740 ppm, respectively, the anomalous catchments were identified (Fig. 5).
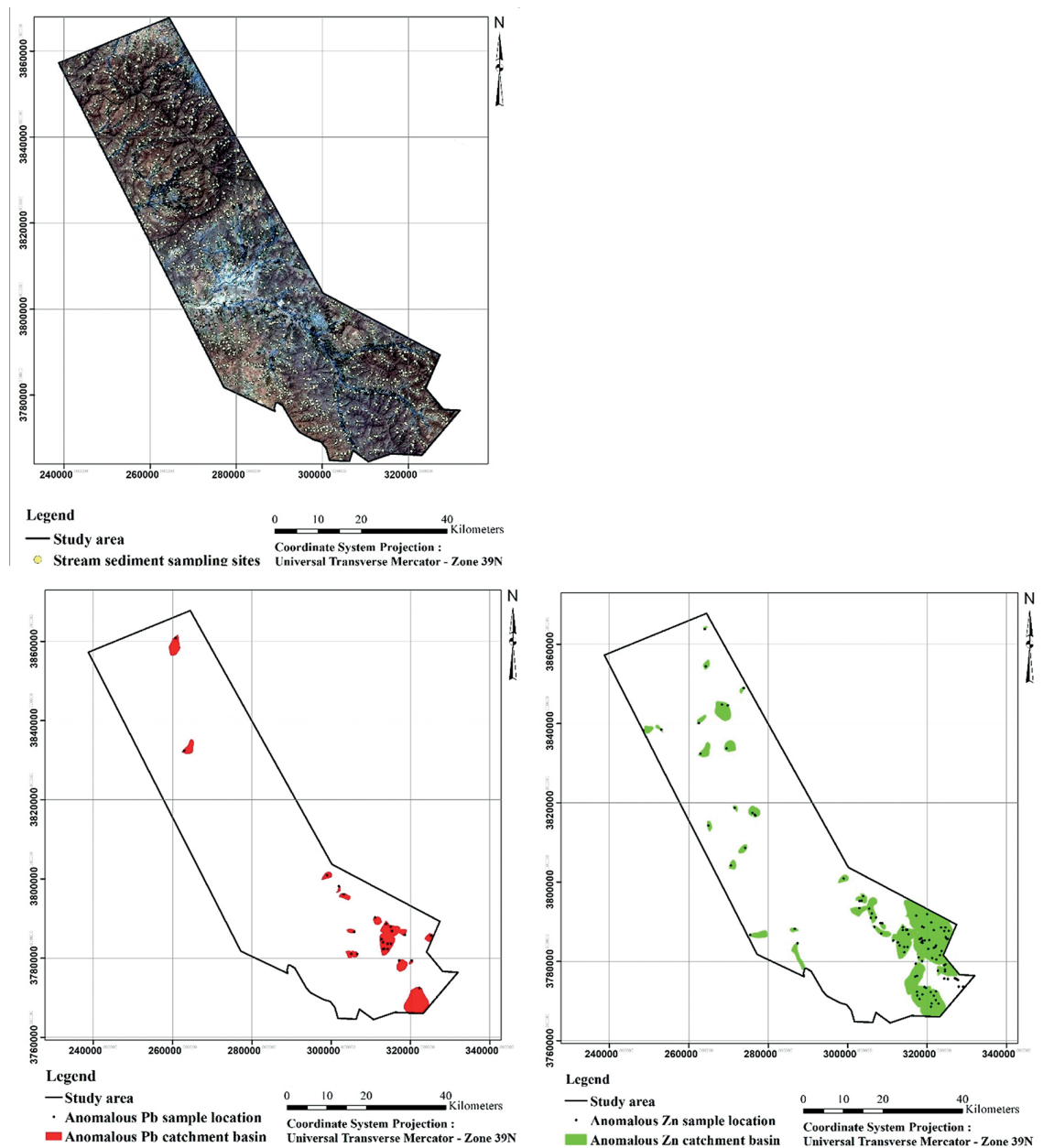
Fig. 5 - Sample catchment basin geochemical map of the elements Pb (left) and Zn (right).

4. Results

A hybrid AHP-TOPSIS method was used to integrate the prepared exploration criteria and produce a final MVT Pb-Zn mineral potential map of the southern Hamedan area. The considered hierarchy structure, based on the input criteria, for MVT Pb-Zn mineralisation in the study area is shown in Fig. 6. It should be noted that the analysis of all the layers prepared in the previous steps was performed on a 200×200 m^2 grid. This choice was made to take into account the dimensions of the geological structures of the study area and to achieve maximum variability. To prepare

the comparison matrices, we asked five Iranian geology experts, familiar with Pb-Zn mineral potential, to create the comparison matrices and send them to us. Then, we used the average of these comparison matrices to determine the weights by the AHP-TOPSIS method. In this way, their opinions influenced the AHP-TOPSIS process. In order to obtain the weight of importance of the four main criteria, first a comparison matrix was created with appropriate *CR* value (*CR* = 0.028). Then, the weight of importance of the individual criteria was calculated through the AHP method (Table 3). The geology, geochemistry, and alteration layers have some sub-criteria whose weights have to be calculated. The comparison matrix of three geological sub-criteria with *CR* = 0.011 was created and the relative weights were obtained using the AHP method (Table 4). The alteration criterion consists of four sublayers, including silicification, iron oxide, propylitic, and argillic alteration. The weights of the importance of these sub-criteria were also determined using the AHP method and based on a pairwise comparison matrix, taking into account the opinion of the geology experts (Table 5). The geochemical layer consists of two sub-criteria, including the Pb and Zn geochemical anomaly map. As in the previous steps, the weights of each geochemical anomaly map were determined using the AHP method (Table 6). To apply the AHP-TOPSIS algorithm, the criteria were first translated into raster maps. Then, using MATLAB scripts developed for AHP-TOPSIS, the relative similarity/closeness to the ideal solution was calculated for each cell of the final raster mineral potential map. Fractal analysis was used to reclassify the final MVT Pb-Zn favourability map into three classes. The thresholds determined by the fractal analysis are shown in Fig. 7. Fig. 8 clearly shows that the known MVT-Pb-Zn deposits are located in or near the highly favourable areas. In addition, several areas of high potential (similar to the known deposits mentioned above) have been identified for further exploration.
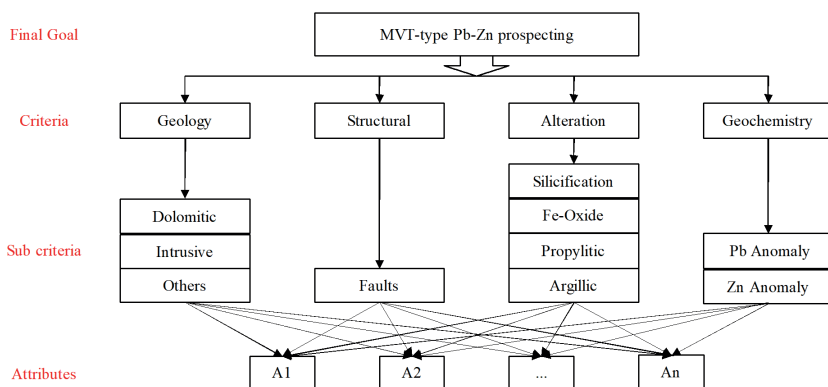
Fig. 6 - The considered hierarchical structure for mapping MVT-Pb-Zn favourability of the southern Hamedan area.

Table 3 - Comparison matrix and obtained weights of the main criteria through AHP method used for MVT Pb-Zn mineral potential mapping.

Criteria	Geology	Structure	Alteration	Geochemistry	Weights
Geology	1	1/2	1/3	1/4	0.10
Structure	2	1	1/2	1/4	0.15
Alteration	3	2	1	1/2	0.27
Geochemistry	4	4	2	1	0.48
CR = **0.028**					

Table 4 - Pairwise comparison matrix and obtained weights of the three geological units through AHP method.

Criteria	Dolomitic rocks	Intrusive rocks	Metamorphic rocks	Weights
Dolomitic rocks	1	3	5	0.61
Intrusive rocks	1/3	1	3	0.29
Metamorphic rocks	1/2	1/3	1	0.10
CR = 0.011				

Table 5 - Pairwise comparison matrix and obtained weights of the four alteration sub criteria through AHP method.

Criteria	Silicification	Fe-Oxide	Propylitic	Argillic	Weights
Silicification	1	1	2	3	0.32
Fe-Oxide	1	1	2	3	0.32
Propylitic	1/2	1/2	1	2	0.19
Argillic	1/3	1/3	2	1	0.17
CR = 0.017					

Table 6 - Pairwise comparison matrix and obtained weights of the two geochemical anomaly maps through AHP method.

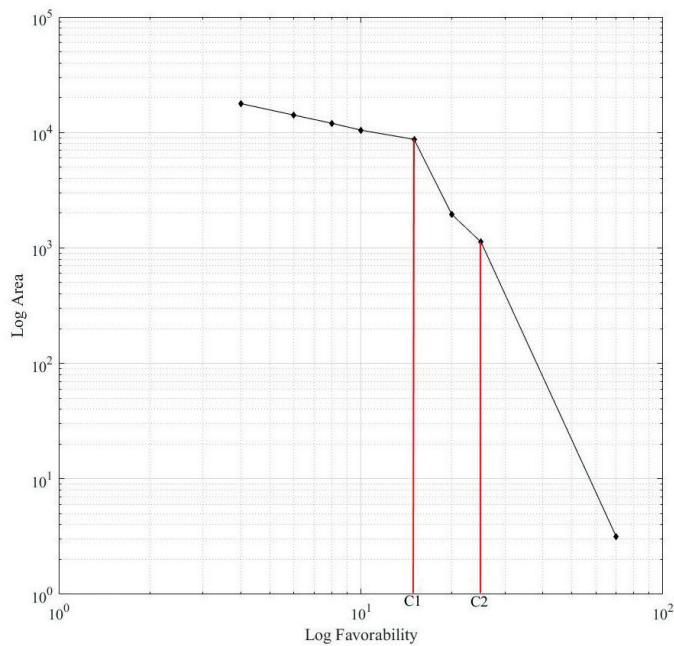| Criteria	Pb	Zn	Weights
Pb	1	2	0.67
Zn	1/2	1	0.33
CR = 0			

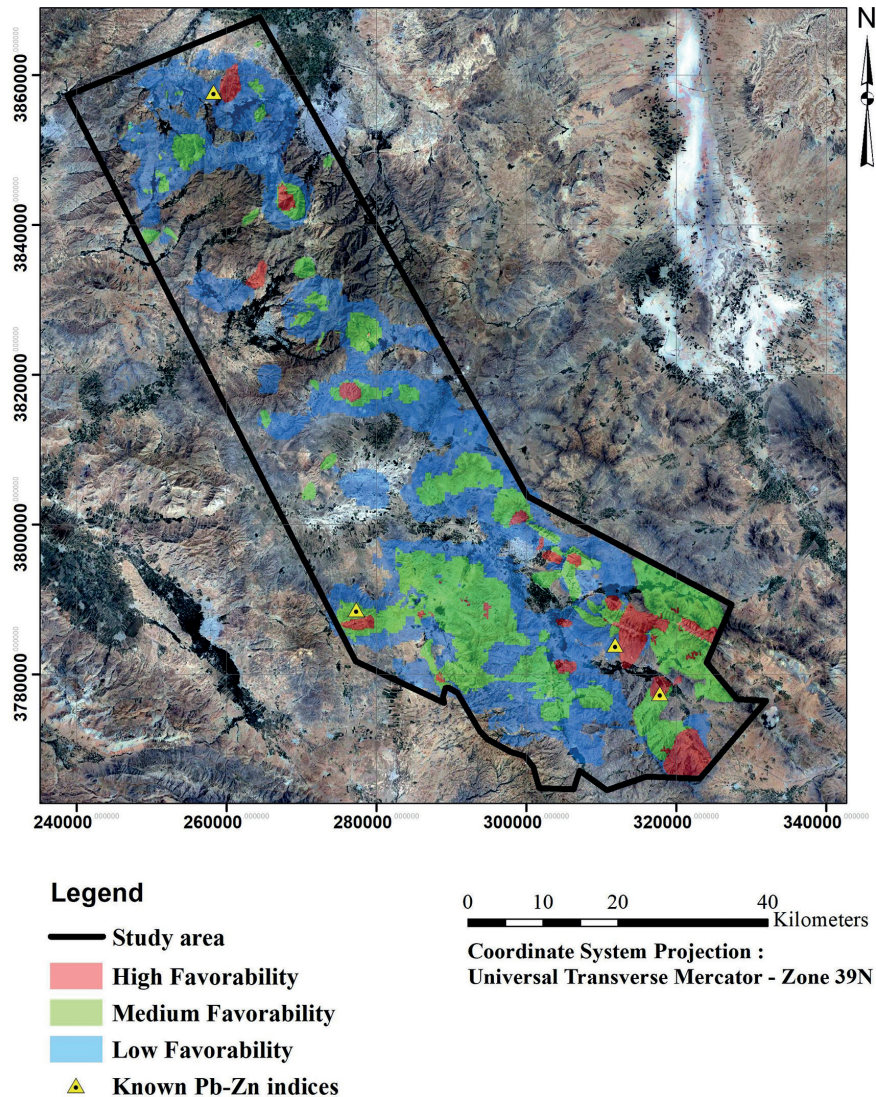Fig. 7 - Log-log diagram of favourability area obtained from the fractal analysis.

Fig. 8 - The classified mineral potential/favourability map was created by integrating various exploration data sets using the AHP-TOPSIS method.

5. Discussion and conclusion

In this article, we have attempted to construct an MVT-Pb-Zn favourability map for a greenfield area with a small number of known Pb-Zn mineralisation indices in the southern Hamedan province of western Iran. This area is part of the Irankuh-Emarate belt, which hosts known MVT Pb-Zn deposits in Iran. For this purpose, an MCDM approach AHP-TOPSIS was used, which is composed of two well-known MCDM algorithms, namely AHP and TOPSIS. In this approach, the relative importance weight of each exploration layer/criterion is calculated based on a pairwise comparison matrix suggested by MVT-Pb-Zn deposit expertise and using the AHP algorithm. In the next step, the pixels of the final favourability raster map are ranked using the TOPSIS

algorithm, whose strategy is similar to both knowledge-based and data-based algorithms. This strategy is based on the calculation of the distance between the alternatives and the positive and negative ideal solutions. The AHP-TOPSIS approach requires only the comparison matrix as input parameters, unlike other algorithms such as fuzzy logic that require more input parameters.

Four main exploration layers, including a 1:100,000 scale geological map, an alteration map, a fault density map, and a map of Pb and Zn geochemical anomalies in the catchment area of the study area, were created and compiled into a final mineralisation potential map.

Through fractal analysis, the final potential map was divided into three classes: highly favourable, favourable, and slightly favourable pixels. The four known prominent Pb-Zn deposits are located in or near the highly favourable pixels. Several unexplored highly favourable and favourable pixels have been identified and are recommended for further exploration.

REFERENCES

Abedi M. and Norouzi G.H.; 2012: *Integration of various geophysical data with geological and geochemical data to determine additional drilling for copper exploration*. J. Appl. Geophys., 83, 35-45.

Abedi M., Torabi S.A., Norouzi G.H. and Hamzeh M.; 2012a: *ELECTRE III: a knowledge-driven method for integration of geophysical data with geological and geochemical data in mineral prospectivity mapping*. J. Appl. Geophys., 87, 9-18.

Abedi M., Torabi S.A., Norouzi G.H., Hamzeh M. and Elyasi G.R.; 2012b: *PROMETHEE II: a knowledge-driven method for copper exploration*. Comput. Geosci., 46, 255-263.

Abedi M., Norouzi G.H. and Fathianpour N.; 2013a: *Fuzzy outranking approach: a knowledge-driven method for mineral prospectivity mapping*. Int. J. Applied Earth Obs. Geoinf., 21, 556-567.

Abedi M., Norouzi G.H. and Torabi S.A.; 2013b: *Clustering of mineral prospectivity area as an unsupervised classification approach to explore copper deposit*. Arabian J. Geosci., 6, 3601-3613.

Agterberg F.P. and Bonham-Carter G.F.; 1999: *October. Logistic regression and weights of evidence modeling in mineral exploration*. In: Proc. 28th International Symposium on Applications of Computer in the Mineral Industry (APCOM), Golden, Colorado, USA, Vol. 483, p. 490.

Amos B.J. and Greenbaum D.; 1989: *Alteration detection using TM imagery The effects of supergene weathering in an arid climate*. Int. J. Remote Sens., 10, 515-527, doi: 10.1080/01431168908903889.

An P., Moon W.M. and Rencz A.; 1991: *Application of fuzzy set theory for integration of geological, geophysical and remote sensing data*. Can. J. Explor. Geophys., 27, 1-11.

Asadi H.H. and Hale M.; 2001: *A predictive GIS model for mapping potential gold and base metal mineralisation in Takab area, Iran*. Comput. Geosci., 27, 901-912.

Asadi H.H., Sansoleimani A., Fatehi M. and Carranza E.J.M.; 2016: *An AHP–TOPSIS predictive model for district-scale mapping of porphyry Cu–Au potential: a case study from Salafchegan area (central Iran).* Natural Resources Research, 25, 417-429.

Bonham-Carter G.F.; 1994: *Geographic information systems for geoscientists: modelling with GIS.* Elsevier, New York, NY, USA, 398 pp.

Bonham-Carter G.F., Agterberg F.P. and Wright D.F.; 1990: *Weights of evidence modelling: a new approach to mapping mineral potential.* In: Agterberg F.P. and Bonham-Carter G.F. (eds), Statistical applications in the earth sciences, Geological Survey of Canada, Ottawa, Canada, pp.171-183, doi: 10.4095/128059.

Boveiri Konari M.; 2016: *Ore-bearing Sulphide facies and genetic model of Detrital-Carbonate-Hosted Zn-Pb mineralisation in the Tappehsorkh deposit, Irankuh mining district, south Esfahan.* Ph.D. Thesis in Geological Sciences, Tarbiat Modares University, Tehran, Iran, 415 pp., in Persian.

Carranza E.J.M.; 2011: *Geocomputation of mineral exploration targets*. Comput. Geosci., 37, 1907-1916.

Carranza E.J.M. and Hale M.; 2001: *Logistic regression for geologically constrained mapping of gold potential, Baguio district, Philippines*. Explor. Min. Geol., 10, 165-175.

Carranza E.J.M. and Laborte A.G.; 2015a: *Data-driven predictive mapping of gold prospectivity, Baguio district, Philippines: application of random forests algorithm*. Ore Geol. Rev., 71, 777-787.

Carranza E.J.M. and Laborte A.G.: 2015b: *Data-driven predictive modeling of mineral prospectivity using random forests: a case study in Catanduanes Island (Philippines)*. Nat. Resour. Res., 25, 35-50.

Carranza E.J.M. and Laborte A.G.; 2015c: *Random forest predictive modeling of mineral prospectivity with small number of prospects and data with missing values in Abra (Philippines)*. Comput. Geosci., 74, 60-70, doi: 10.1016/j.cageo.2014.10.004.

Carranza E.J.M., Mangaoang J.C. and Hale M.; 1999: *Application of mineral exploration models and GIS to generate mineral potential maps as input for optimum land-use planning in the Philippines*. Nat. Resour. Res., 8, 165-173.

Carranza E.J.M., Hale M. and Faassen C.; 2008: *Selection of coherent deposit-type locations and their application in data-driven mineral prospectivity mapping*. Ore Geol. Rev., 33, 536-558.

Ehya F., Lotfi M. and Rasa I.; 2010: *Emarat carbonate-hosted Zn-Pb deposit, Markazi Province, Iran: a geological, mineralogical and isotopic (S, Pb) study*. J. Asian Earth Sci., 37, 186-194.

Feizi F. and Mansuri E.; 2013: *Separation of alteration zones on ASTER data and integration with drainage geochemical maps in Soltanieh, northern Iran*. Open J. Geol., 3, 134-142, doi: 10.4236/ojg.2013.32017.

Ford A., Miller J.M. and Mol A.G.; 2016: *A comparative analysis of weights of evidence, evidential belief functions, and fuzzy logic for mineral potential mapping using incomplete data at the scale of investigation*. Nat. Resour. Res., 25, 19-33, doi: 10.1007/s11053-015-9263-2.

Gabr S., Ghulam A. and Kusky T.; 2010: *Detecting areas of high-potential gold mineralisation using ASTER data*. Ore Geol. Rev., 38, 59-69.

Galvão L.S., Almeida-Filho R. and Vitorello Í.; 2005: *Spectral discrimination of hydrothermally altered materials using ASTER short-wave infrared bands: evaluation in a tropical savannah environment*. Int. J. Appl. Earth Obs. Geoinf., 7, 107-114, doi: 10.1016/j.jag.2004.12.003.

Geranian H., Tabatabaei S.H., Asadi H.H. and Carranza E.J.M.; 2016: *Application of discriminant analysis and support vector machine in mapping gold potential areas for further drilling in the Sari-Gunay gold deposit, NW Iran*. Nat. Resour. Res., 25, 145-159, doi: 10.1007/s11053-015-9271-2.

Ghezelbash R. and Maghsoudi A.; 2018: *A hybrid AHP-VIKOR approach for prospectivity modeling of porphyry Cu deposits in the Varzaghan District, NW Iran*. Arabian J. Geosci., 11, 1-15.

Honarmand M., Ranjbar H. and Shahabpour J.; 2012: *Application of principal component analysis and spectral angle mapper in the mapping of hydrothermal alteration in the Jebal-Barez area, southeastern Iran*. Resour. Geol., 62, 119-139.

Hosseinali F. and Alesheikh A.A.; 2008: *Weighting spatial information in GIS for copper mining exploration*. Am. J. Appl. Sci., 5, 1187-1198.

Hwang C.L. and Yoon K.; 1981: *Methods for multiple attribute decision making.* In: Hwang C.L. and Yoon K. (eds), Multiple attribute decision making: methods and applications a state-of-the-art survey, Lecture Notes in Economics and Mathematical Systems, vol. 186, Springer, Berlin, Heidelberg, Germany, vol. 186, pp. 58-191, doi: 10.1007/978-3-642-48318-9_3.

Jahanshahloo G.R., Lotfi F.H. and Izadikhah M.; 2006: *An algorithmic method to extend TOPSIS for decision-making problems with interval data*. Appl. Math. Comput., 175, 1375-1384.

Karimpour M.H. and Sadeghi M.; 2018: *Dehydration of hot oceanic slab at depth 30-50 km: KEY to formation of Irankuh-Emarat PbZn MVT Belt, central Iran*. J. Geochem. Explor., 194, 88-103.

Lai Y.J., Liu T.Y. and Hwang C.L.; 1994: *Topsis for MODM*. Eur. J. Oper. Res., 76, 486-500.

Mahmoodi P., Rastad E., Rajabi A. and Peter J.M.; 2018: *Ore facies, mineral chemical and fluid inclusion characteristics of the Hossein-Abad and Western Haft-Savaran sediment-hosted Zn-Pb deposits, Arak Mining District, Iran.* Ore Geology Reviews, 95, 342-365.

McKay G. and Harris J.R.; 2016: *Comparison of the data-driven random forests model and a knowledge-driven method for mineral prospectivity mapping: a case study for gold deposits around the Huritz group and Nueltin suite, Nunavut, Canada*. Nat. Resour. Res., 25, 125-143, doi: 10.1007/s11053-015-9274-z.

Movahednia M., Rastad E., Rajabi R. and González F.J.; 2018: *Evidence for syn-sedimentary faulting and reduced formation environment of the Ab-Bagh SEDEX-type Zn-Pb deposit, south of Shahreza, Sanandaj-Sirjan zone*. Sci. Q. J. Geosci., 27, 233-244.

Niroomand S., Haghi A., Rajabi A., Shabani A.A.T. and Song Y.C.; 2019: *Geology, isotope geochemistry, and fluid inclusion investigation of the Robat Zn-Pb-Ba deposit, Malayer-Esfahan metallogenic Belt, southwestern Iran*. Ore Geol. Rev., 112, 17 pp., doi:10.1016/J.OREGEOREV.2019.103040.

Opricovic S. and Tzeng G.H.; 2004: *Compromise solution by MCDM methods: a comparative analysis of VIKOR and TOPSIS.* Eur. J. Oper. Res., 156, 445-455.

Pazand K. and Hezarkhani A.; 2015: *Porphyry Cu potential area selection using the combine AHP-TOPSIS methods: a case study in Siahrud area (NW, Iran)*. Earth Sci. Inf., 8, 207-220.

Pazand K., Hezarkhani A., Ataei M. and Ghanbari Y.; 2011: *Combining AHP with GIS for predictive Cu porphyry potential mapping: a case study in Ahar area (NW, Iran)*. Nat. Resour. Res., 20, 251-262.

Pazand K., Hezarkhani A. and Ataei M.; 2012: *Using TOPSIS approaches for predictive porphyry Cu potential mapping: a case study in Ahar-Arasbaran area (NW, Iran)*. Comput. Geosci., 49, 62-71.

Peernajmodin H.; 2018: *Ore facies, geochemistry and genesis of Zn-Pb-Ba and Fe carbonatehosted Khan-Abad, KuhKolangeh, Robat and Shams-Abad deposit, south Arak area*. Ph.D. Thesis in Geological Sciences, Tarbiat Modares University, Tehran, Iran, unpublished.

Porwal A., Carranza E.J.M. and Hale M.; 2003a: *Artificial neural networks for mineral-potential mapping: a case study from Aravalli province, western India*. Nat. Resour. Res., 12, 155-171.

Porwal A., Carranza E.J.M. and Hale M.; 2003b: *Knowledge-driven and data-driven fuzzy models for predictive mineral potential mapping*. Nat. Resour. Res., 12, 1-25.

Pournamdari M., Hashim M. and Pour A.B.; 2014: *Application of ASTER and landsat TM data for geological mapping of Esfandagheh Ophiolite complex, southern Iran*. Res. Geol., 64, 233-246.

Rajabi A., Mahmoodi P., Rastad E., Niroomand S., Canet C., Alfonso P., Shabani A.A.T. and Yarmohammadi A.; 2019: *Comments on "Dehydration of hot oceanic slab at depth 30-50 km: key to formation of Irankuh-Emarat Pb-Zn MVT Belt, central Iran" by Mohammad Hassan Karimpour and Martiya Sadeghi*. J. Geochem. Explor., 205, 106346, 10 pp.

Saaty T.L.; 1977: *A scaling method for priorities in hierarchical structures*. J. Math. Psychology, 15, 234-281.

Saaty T.L.; 1980: *The analytic hierarchy process: planning, priority setting. Resource allocation*. McGraw-Hill, New York, NY, USA, 287 pp.

Saaty T.L.; 1994: *Fundamentals of decision making and priority theory with the analytic hierarchy process*. RWS Publications, Pittsburgh, PA, USA, 477 pp.

Saaty T.L.; 1997: *That is not the analytic hierarchy process: what the AHP is and what it is not.* Journal of Multi-Criteria Decision Analysis, 6, 324-335.

Saaty T.L.; 2001: *Fundamentals of the analytic hierarchy process.* In: Schmoldt D.L., Kangas J., Mendoza G.A. and Pesonen M. (eds), The analytic hierarchy process in natural resource and environmental decision making, Managing Forest Ecosystems, Springer, Dordrecht, The Netherlands, vol. 3, pp. 15-35, doi: 10.1007/978-94-015-9799-9_2.

Shahriari H., Ranjbar H. and Honarmand M.; 2013: *Image segmentation for hydrothermal alteration mapping using PCA and concentration-area fractal model*. Nat. Resour. Res., 22, 191-206.

Tzeng G.H. and Huang J.J.; 2011: *Multiple attribute decision making: methods and applications, 1st ed*. Chapman and Hall/CRC, New York, NY, USA, 352 pp., doi: 10.1201/b11032.

Yarmohammadi A.; 2015: *Origin and characteristics of ore forming fluids and genetic model of carbonate hosted Zn-Pb deposits in upper part of lower cretaceous sequence, north Tiran basin in NW of Esfahan*. Ph.D. Thesis in Geological Sciences, Tarbiat Modares University, Tehran, Iran, 395 pp., unpublised.

Yoon K.P. and Hwang C.L.; 1995: *Multiple attribute decision making: an introduction*. Sage Publications, Thousand Oaks, CA, USA, vol. 104, 73 pp.

Yousefi M. and Carranza E.J.M.; 2015: *Geometric average of spatial evidence data layers: a GIS-based multi-criteria decision-making approach to mineral prospectivity mapping*. Comput. Geosci., 83, 72-79.

Corresponding author: Hooshang Asadi Haroni
Department of Mining Engineering, Isfahan University of Technology
3rd Abshar, 8415683111 Isfahan, Iran
Phone: +98 913 402 8040, e-mail: hooshang@cc.iut.ac.ir